JACS
JOURNAL OF THE AMERICAN CHEMICAL SOCIETY
Article
pubs.acs.org/JACS

# Bottom-Up Synthesis of Soluble and Narrow Graphene Nanoribbons Using Alkyne Benzannulations

Wenlong Yang,[†] Andrea Lucotti,[‡] Matteo Tommasini,[‡] and Wesley A. Chalifoux*[,†]

[†]Department of Chemistry, University of Nevada, Reno, Nevada 89557-0216, United States

[‡]Dipartimento di Chimica, Materiali e Ingegneria Chimica "G. Natta,", Politecnico di Milano, Piazza Leonardo da Vinci 32, 20133 Milano, Italy

Supporting Information

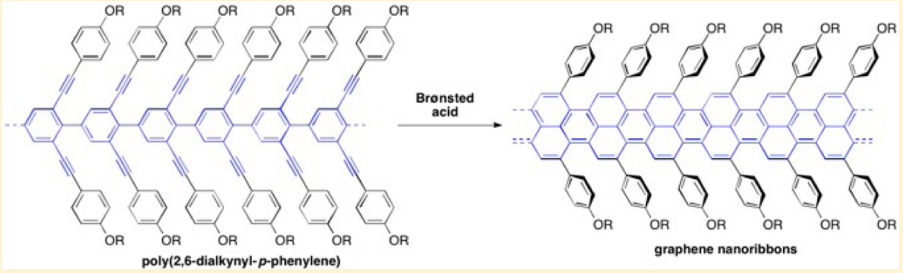


**ABSTRACT:** Since the discovery of graphene, there is an increasing amount of research devoted to graphene materials, namely, graphene nanoribbons (GNRs). The "top-down" production of narrow (<10 nm wide), unoxidized, and easily processable GNRs with atomically precise edges is challenging, and therefore, new methods need to be developed. We have designed a "bottom-up" approach for the synthesis of very narrow (ca. 0.5 nm) and soluble GNRs using a nonoxidative alkyne benzannulation strategy promoted by Brønsted acid. Suzuki polymerization was used to produce the GNR precursor, a poly(2,6-dialkynyl-*p*-phenylene) (PDAPP), with a weight-average molecular weight of 37.6 kg mol$^{-1}$. Cyclization of the ethynylaryl side chains on PDAPP was efficiently achieved using Brønsted acids to ultimately produce the GNRs. Infrared and Raman spectroscopic characterization of the GNRs matches very well with calculated results. The formation of the GNRs was also supported by transmission electron microscopy (TEM) and scanning tunneling microscopy (STM).

## INTRODUCTION

Graphene, an organic material comprised of a two-dimensional monolayer of sp$^2$-hybridized carbon atoms, has been shown to have interesting electronic, thermal, mechanical, and optical properties.[1−3] Its use in some important applications, like field effect transistors (FETs), is not possible because it is a zero bandgap semiconductor. Opening the bandgap can be achieved by producing narrow strips of graphene, known as graphene nanoribbons (GNRs).[4−7] A number of "top-down" approaches, such as the scission of graphene sheets using lithography,[8−10] plasma etching,[11] or the "unzipping" of carbon nanotubes,[12−15] can provide GNRs. These methods commonly produce impure GNRs as a mixture of different sizes and shapes with poor solubility, which complicates processing of the materials for device applications. In addition, the harsh conditions used in these top-down methods can result in poor-quality GNRs, which affects their properties and limits their use in device applications. A more rational way to produce pure GNRs is through a total synthesis from simple starting materials (i.e., a "bottom-up" approach). This would allow for better control of the size, shape, and functionalization of the GNRs, leading to improved solubility and material properties.

GNRs are predicted to have metallic to semiconducting properties, and those with widths <10 nm should possess ideal semiconducting properties for FET applications.[6,16,17] Some excellent bottom-up approaches toward GNRs have been reported. Müllen and co-workers recently reported the solution-phase synthesis of soluble GNRs > 200 nm's long using a Diels−Alder polymerization reaction.[18] Chevron-type GNRs that are all carbon[19,20] and also nitrogen-doped[21] have also been made by solution-phase synthesis. These approaches rely upon oxidative aryl−aryl bond formation (the Scholl reaction) for key C−C bond forming reactions,[18−29] but the harsh conditions that are required can significantly limit the functionality that can be incorporated into the GNRs. This, in turn, limits the ability to tune the properties of the resulting GNR through the incorporation of various substituents. Undesired rearrangements are also possible under Scholl reaction conditions.[30] The bottom-up synthesis of very narrow and atomically precise GNRs has also been accomplished oxidatively on a Au(111) surface[17,31−35] and also a Cu(111) surface.[36,37] A drawback of surface-assisted synthesis of GNRs is that this methodology is currently not practical for producing bulk quantities of soluble and processable GNRs. New methodologies are therefore needed for the efficient and

**Received:** March 23, 2016
**Published:** June 29, 2016





DOI: 10.1021/jacs.6b03014
J. Am. Chem. Soc. 2016, 138, 9137−9144

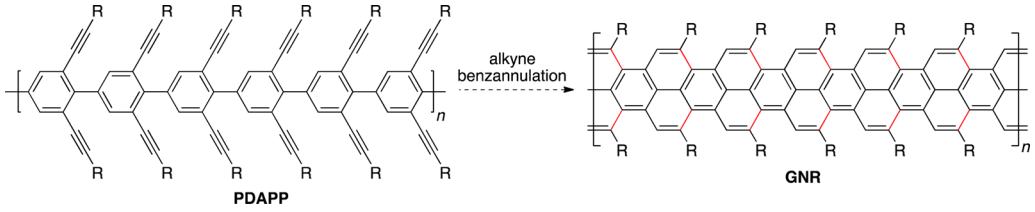


**Figure 1.** Bottom-up synthesis of GNRs via an alkyne benzannulation strategy.

rational bottom-up synthesis of narrow and soluble GNRs in appreciable quantities so that further studies on this material is possible.

The bottom-up synthesis of soluble and narrow GNRs in appreciable quantities is still an unmet challenge. Therefore, the development of synthetic methods to provide bulk quantities of GNRs less than 10 nm wide would be highly beneficial since these narrow GNRs would contain a bandgap, which is necessary in FET applications. In theory, this bandgap could be tuned by adjusting the width of the GNR or though substituent effects. Herein, we report a new bottom-up synthesis narrow GNRs based on a Brønsted acid promoted alkyne benzannulation of a linear poly(2,6-dialkynyl-*p*-phenylene) (PDAPP) precursor (Figure 1). The GNR products are highly soluble in a number of common organic solvents. The structure of the GNRs were supported by gel permeation chromatography (GPC), nuclear magnetic resonance (NMR), infrared, Raman, and ultraviolet−visible−near infrared (UV−vis−NIR) spectroscopies as well as transmission electron microscopy (TEM) and scanning tunneling microscopy (STM).

## RESULTS AND DISCUSSION

**Model Study.** The cyclization of alkyne substituents onto aryl moieties (benzannulation) has been shown to be an efficient and mild method to generate a new aryl rings. This can be achieved by using a variety of $\pi$-Lewis acids,[38−40] using iodine monochloride[41] and even some Brønsted acids.[42−44] In order to evaluate the feasibility for PDAPP benzannulation, a model compound (MC) was synthesized that represents a monomeric unit of PDAPP (Scheme 1). The cyclization of 2,6-dialkynebiphenyl derivative **MC1** was tested using a number of conditions to generate pyrene **MC2**.[45] In our hands, the use of $\pi$-Lewis acids or ICl[46] resulted in incomplete cyclization or poor yields of pyrene products via a double benzannulation of 2,6-dialkynylbiphenyl derivatives. We then turned our attention to Brønsted acids to promote the cyclization reaction. Compound **MC1** gives the monobenzannulated product **MC3** almost quantitatively in the presence of excess trifluoroacetic acid (TFA) at room temperature. Doubly benzannulated pyrene product **MC2** can be obtained in low yield after long reaction times at reflux in the presence of excess TFA. It appeared that the second cyclization step was much more difficult, and it appeared that a stronger Brønsted acid would be required. Conducting the cyclization reaction using methanesulfonic acid (MSA) provided compound **MC2** in 85% yield (see the Supporting Information). We found that the use of excess strong acid, such as MSA or triflic acid, significantly accelerated the double benzannulation reaction but also led to the formation of an uncharacterized byproduct. The best conditions consisted of effecting a clean monocylization at room temperature first using excess TFA, followed by transferring this reaction mixture via syringe pump into a solution of triflic acid (1 equiv) at low temperature to give **MC2** in excellent yield. We have also demonstrated that this method works well for the synthesis of larger polycyclic aromatic hydrocarbons (PAHs), such as pero- and teropyrenes, via a 2- and 4-fold alkyne benzannulation, respectively.[45]

**Scheme 1. Model Study for the Brønsted Acid Catalyzed Double Benzannulation of MC1 to MC2**

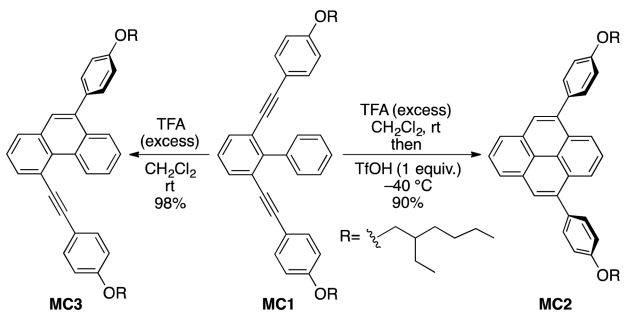


**Synthesis of GNRs.** Our synthesis of GNRs started with the conversion of aniline **1** to the triazene compound **2** followed by selective double Sonogashira crosscoupling with alkyne **3** to afford dialkynyltriazene **4** (Scheme 2). Conversion of the triazene **4** to the bromoiododialkynylbenzene **5** was achieved in good yield using known conditions.[47] Compound **5** underwent selective lithium−halogen exchange using butyllithium and was carried on to boronic acid **6** in good yield. We converted **6** to the pinacol boronate **7** as it was easier to purify and also provided higher molecular weight polymers in the polymerization step (vide infra). With monomer **7** in hand, we prepared a linear PDAPP **8** using a Suzuki cross-coupling polymerization reaction. Branched alkyl chains were incorporated into monomer **7** to enhance the solubility of the PDAPP **8** and GNR **9** products. The crude PDAPP product **8** was taken up in minimal hexane, precipitated with methanol, and then analyzed by GPC against polystyrene (PS) standards. It should be noted that the calculated molecular weights obtained from GPC analysis are only an estimate to get an approximate idea of the GNR lengths after cyclization and the values reported here may deviate from values obtained from light scattering experiments. The results indicated that PDAPP **8a** (produced in toluene) had a weight-average molecular weight ($M_w$) of 8.9 kg mol$^{-1}$. The choice of reaction solvent (toluene vs THF) makes a tremendous difference on the molecular weights obtained after polymerization where PDAPP **8b** (produced in THF) had a significantly higher $M_w$ of 37.6 kg mol$^{-1}$ (see Supporting Information, Table S1). The polydispersity index (PDI) was 1.6 for **8a** and 1.4 for **8b**. To our surprise, nearly complete benzannulation of PDAPP **8** was observed after 24 h using excess TFA at room temperature (see the Supporting Information). Although significant cyclization of PDAPP **8** was observed according to the $^1$H NMR, complete cyclization cannot be achieved using TFA, even if excess acid is used. We


DOI: 10.1021/jacs.6b03014
J. Am. Chem. Soc. 2016, 138, 9137−9144

**Scheme 2. Synthesis of PDAPP 8 and Its Benzannulation to Form GNR 9**

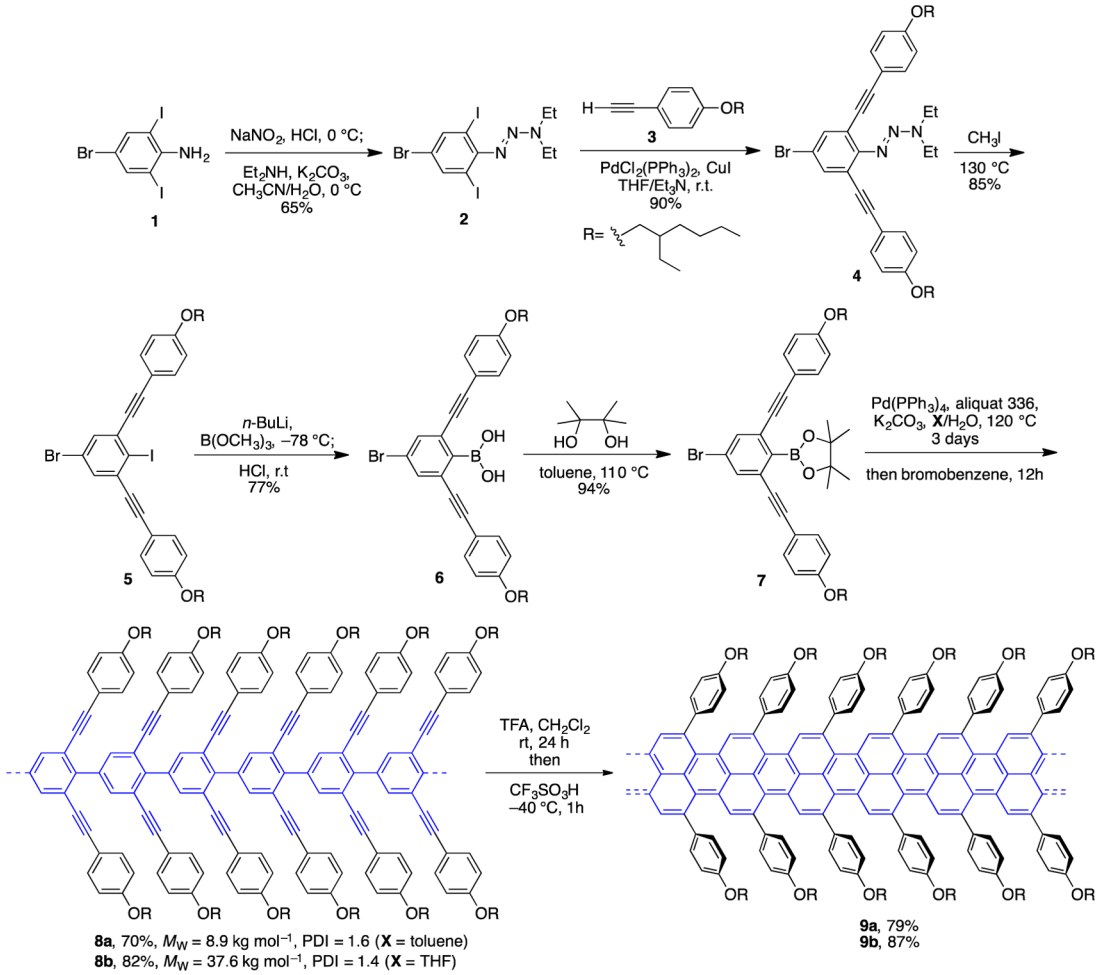


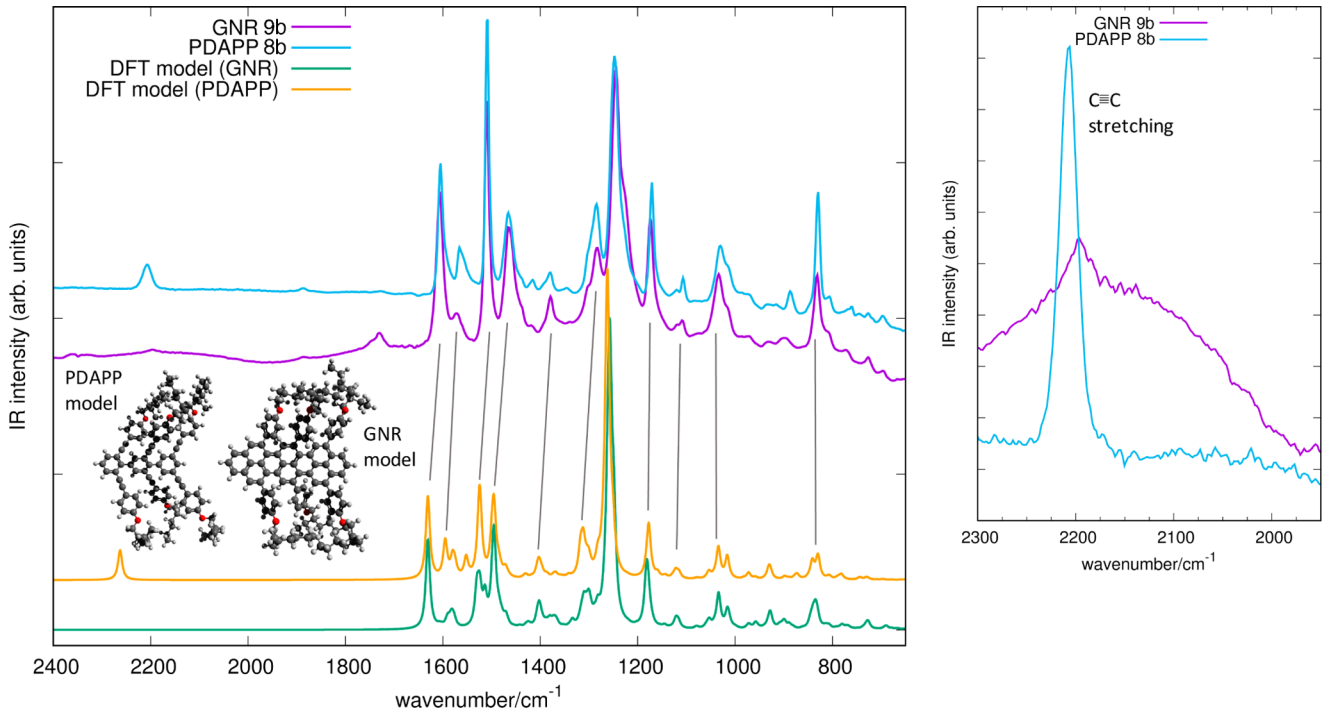


**Figure 2.** Experimental (blue and purple) IR spectra of PDAPP **8b**, GNR **9b**, and simulated spectra (yellow and green). The right panel shows an expansion of the CC triple bond stretching region where the intensity of the GNR **9b** has been increased to improve clarity.



DOI: 10.1021/jacs.6b03014
J. Am. Chem. Soc. 2016, 138, 9137–9144

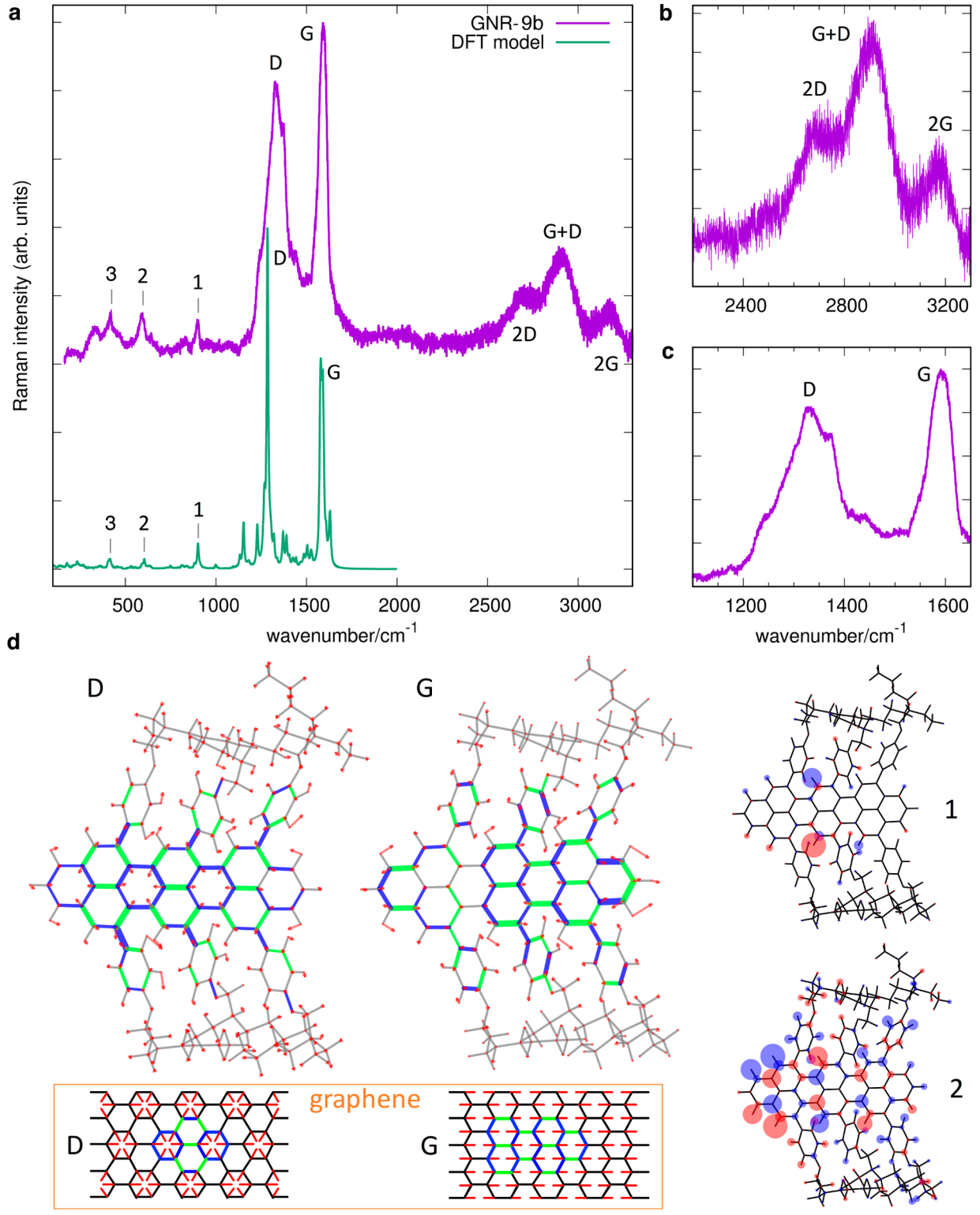


**Figure 3.** (a) Experimental and simulated Raman spectrum of GNR **9b**; (b,c) direct comparison of the first and the second-order experimental Raman spectrum, which allows a straightforward identification of overtones and combinations. In panel d, the relevant Raman lines have been labeled, and selected nuclear displacements are reported. To help the reader in recognizing the characteristic D and G nuclear displacement patterns, the corresponding modes of graphene are displayed (orange rectangle, adapted from ref 51). In the sketch of the normal modes, red arrows represent displacement vectors; CC bonds are represented as green (blue) lines of different thickness according to their relative stretching (shrinking). For modes 1 and 2 (right-hand side of panel d), the sizes of blue/red circles of the molecular sketch are proportional to nuclear displacements in the out-of-plane direction.

were successful in driving the cyclization reaction to completion by using triflic acid at −40 °C, resulting in 79% and 87% yield of **9a** and **9b**, respectively. The average lengths of **9a** and **9b** are estimated to be about 8 and 35 nm, respectively, and are



DOI: 10.1021/jacs.6b03014
J. Am. Chem. Soc. 2016, 138, 9137−9144

calculated based on the $M_w$ of the PDAPP precursors **8a** and **8b**. There was very little change in the molecular weight distribution when going from PDAPP **8** to GNR **9**, which suggests that there were minimal to no intermolecular reactions that occurred during the benzannulation reaction.

**Infrared (IR) Spectroscopic Characterization.** The IR spectra of PDAPP **8b** and GNR **9b** were analyzed and compared with the results from DFT calculations (Figure 2). The overall spectral pattern of PDAPP **8b** and GNR **9b** are quite similar, with the notable exception of the CC stretching of the triple bonds, which is observed around 2200 $cm^{-1}$. In fact, the conversion from PDAPP **8b** to GNR **9b** requires that the triple bonds be converted into conjugated double bonds making up the GNR backbone. Interestingly, one can notice a very weak signal (2196 $cm^{-1}$) in the IR spectrum of GNR **9b** that is attributed to CC stretching of unreacted triple bonds, but this signal is red-shifted compared to that of PDAPP **8b** (2206 $cm^{-1}$). This red-shift can be rationalized by a DFT model of a partially reacted GNR that still contains a triple bond and now is connected to a highly conjugated system (see Supporting Information, Figure S11). The fact that the strength of this signal compares with that of overtones/combinations of aromatic systems in the 1700−2000 $cm^{-1}$ region[48,49] is an indication of the intrinsic weakness of this signal in the GNR **9b** sample. This means that the number of unreacted CC triple bonds is small.

The remaining part of the fingerprint region is remarkably similar in PDAPP **8b** and GNR **9b**, both in the experimental results and the DFT simulations. In fact, the chemical structure of both systems overlaps to a good extent. Notably, the side groups are the same in PDAPP **8b** and GNR **9b** and carry polar CO bonds which are known to promote strong IR bands.[48] Consistently, DFT calculations reveal that the strong signal observed at 1246 $cm^{-1}$ is due to CO stretching coupled with CH wagging of the aryl side groups. Similarly, DFT calculations allow us to assign the IR band at 1606 $cm^{-1}$ to ring stretching of the aryl side groups. The IR band at 1510 $cm^{-1}$ is attributed to in-plane CH bending at the aryl side groups and $-CH_2-$ scissoring. The band at 831 $cm^{-1}$ is due to the collective out-of-plane CH bending of the aryl side groups.

**Raman Spectroscopic Characterization.** The Raman spectroscopic data for GNR **9b** was obtained with 514.5 nm excitation (Figure 3a−c). The expected G (1592 $cm^{-1}$) and D (1332 $cm^{-1}$) signatures of GNR[50] are clearly observed after baseline correction (see Supporting Information, Figure S12). The related overtones and combinations (2D, 2690 $cm^{-1}$; G + D, 2906 $cm^{-1}$; 2G, 3179 $cm^{-1}$) are also observed, similar to other reported GNRs.[27] DFT calculations of the first-order Raman spectrum of a model molecule composed by three translational units of GNR (Figure 3d) favorably compare with the experimental data (see Figure 3a) and support the assignment of the G and D signals to the expected nuclear displacement patterns, as compared with graphene (orange rectangle, Figure 3d).[51] Furthermore, the low wavenumber region of the Raman spectrum (<1000 $cm^{-1}$) displays three interesting lines which DFT calculations assign to (1) CH out-of-plane bending at the GNR edge (897 $cm^{-1}$); (2) coupled out-of-plane bending of the GNR backbone and CH bonds (590 $cm^{-1}$); (3) collective deformation of the GNR backbone with complex pattern (417 $cm^{-1}$, see Supporting Information, Figure S13). A comparison to the FT-Raman spectrum of the precursor molecule PDAPP **8b** shows the disappearance of the line at about 2200 $cm^{-1}$ (attributed to the CC stretching of the triple bonds) and indicates that the cyclization reaction occurred at these sites. The observed IR and Raman spectra and their very good match against DFT calculations on a suitable molecular model support the successful synthesis of GNR **9b**.

**NMR and UV−Visible−NIR Spectroscopic Characterization.** The conversion of PDAPP **8** to GNR **9** was confirmed also by nuclear magnetic resonance (NMR) and UV−vis−NIR spectroscopies (Figure 4). The $^1H$ NMR spectrum showed broad signals and was less informative than the $^{13}C$ NMR spectrum. Analysis by $^{13}C$ NMR spectroscopy showed clean conversion of PDAPP **8** to GNR **9** by the disappearance of the PDAPP alkyne signals (88.1 and 94.1 ppm, blue circles, Figure 4a; MC1 and MC2 included for comparison). The diagnostic

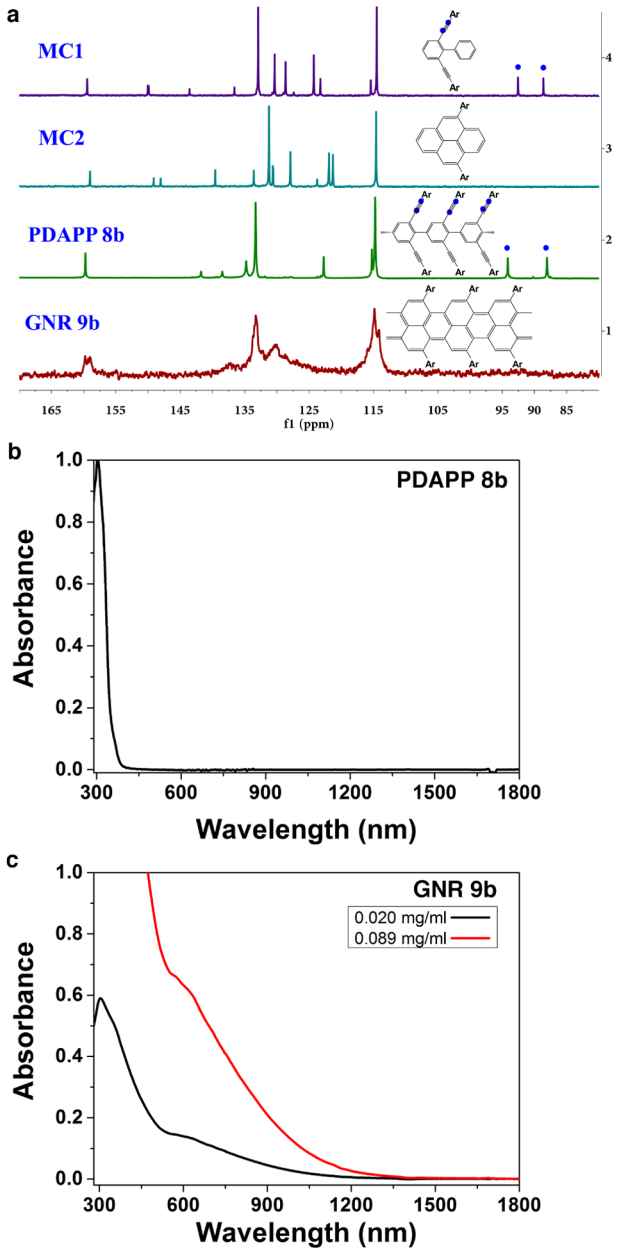


**Figure 4.** (a) Comparison of $^{13}C$ NMR spectra for **MC1**, **MC2**, PDAPP **8b**, and GNR **9b** showing the disappearance of alkyne signals (blue dots) supporting the conversion of PDAPP **8b** to GNR **9b**. (b) UV−vis−NIR spectra of PDAPP **8b** and (c) GNR **9b**.



DOI: 10.1021/jacs.6b03014
J. Am. Chem. Soc. 2016, 138, 9137−9144

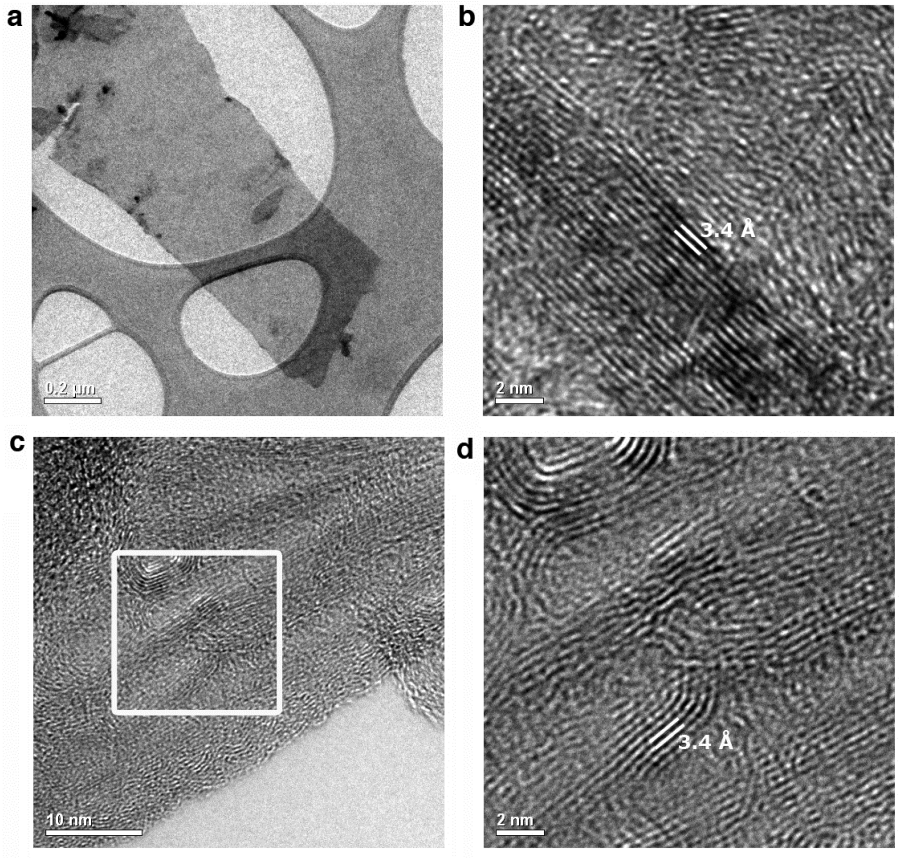


**Figure 5.** Characterization of GNRs by TEM using $RuO_4$ staining for higher contrast. (a) Low-magnification TEM image showing a thin sheet of aggregated GNRs (black regions are high concentrations of $RuO_4$). (b) High-resolution (HR) TEM image of the GNRs showing long linear strands aggregated together with the distance between layers being 3.4 Å. (c) HRTEM image showing curved regions of GNRs, demonstrating their flexibility. (d) Expanded region (white square) of curved GNRs.

signal around 10.5 ppm (from the hydrogen in the 5-position of MC3) in the $^1$H NMR spectrum that arises from partial cyclization was nearly absent, confirming nearly complete cyclization, as was also seen by IR spectroscopic analysis (see Figure 2 and the Supporting Information for details).

The PDAPP and GNRs were also characterized by UV–vis–NIR spectroscopic analysis (Figures 4b and c). The absorbance spectrum of PDAPP **8b** (Figure 4b) in $CH_2Cl_2$ solution shows a relatively high energy and sharp absorbance ($\lambda_{max}$ = 309 nm). After benzannulation, we observed that GNR **9b** broadly absorbs from the UV region beyond the visible region and into the near-IR (Figure 4c). The low-energy absorbance band is broad due to the superposition of GNRs with various MWs. The spectrum has a similar appearance to known GNRs and appears to have a maximum absorbance roughly around 700 nm, which is slightly red-shifted when compared to wider GNRs.[18,28,29] GNR 9b begins to significantly absorb starting at ~1200 nm, corresponding to an optical bandgap of approximately 1.03 eV.

**Microscopy.** Transmission electron microscopy (TEM) was conducted on GNR **9b**. The sample was dispersed in methanol (no sonication was used), deposited on lacey carbon grids, and then stained with $RuO_4$ to improve the contrast of the images (Figure 5). At low magnification, the GNRs consisted of one large thin film that likely arises from agglomeration during solvent evaporation (Figure 5a); The HRTEM images showed areas with layers of GNRs with a distance between layers of 3.4 Å (Figure 5b–d). This is consistent with the interlayer distances observed for other GNRs[52,53] and similar to that of few-layered graphene[54] and pristine graphite.[55] The area with curving layers demonstrates just how flexible the GNRs are (Figure 5c and d).

We also obtained molecular resolution scanning tunneling microscopy (STM) images of GNR **9b** at the solid–liquid interface of highly oriented pyrolytic graphite (HOPG) (see Supporting Information, Figures S16 and S17). The STM images of GNR **9b** show the expected one-dimensionality of the ribbons and regularity along the chain axis with a measured width of ~3.4 nm, which is in agreement with the calculated width. The STM images also show that there are some GNRs that contain defects in which branching of the GNR has occurred.

## ■ CONCLUSIONS

In summary, we have demonstrated that alkyne benzannulation promoted by Brønsted acid is a viable method for the bottom-up synthesis of narrow and soluble GNRs. The polymerization of the monomer results in polymers of ca. 70 repeat units in length, on average. This poly(*p*-phenylene) intermediate (PDAPP) can be subjected to a number of different acids (TFA, methanesulfonic acid, or triflic acid) to promote the cyclization reaction resulting in GNRs. The GNRs show remarkable flexibility, as seen by STM and TEM analysis.


DOI: 10.1021/jacs.6b03014
J. Am. Chem. Soc. 2016, 138, 9137–9144

## ■ ASSOCIATED CONTENT

### Supporting Information

The Supporting Information is available free of charge on the ACS Publications website at DOI: 10.1021/jacs.6b03014.

Experimental procedures, NMR spectra, supplementary STM images, and supplementary UV−vis, IR, and Raman spectra (PDF)

## ■ AUTHOR INFORMATION


### Corresponding Author

*wchalifoux@unr.edu


### Notes

The authors declare no competing financial interest.

## ■ ACKNOWLEDGMENTS

Acknowledgment is made to the Donors of the American Chemical Society Petroleum Research Fund for support of this research (PRF No. 53543-DNI1). This work was partly supported by startup funds from the University of Nevada, Reno. We also thank the National Science Foundation for support through a CAREER Award (CHE-1555218). We thank our colleagues Prof. B. T. King for insightful discussions, D. Murray for training W.Y. on STM as well as his assistance in acquiring some of the STM images, Prof. J. Shearer for access to instrumentation and helping us acquire UV−vis−NIR spectra, Dr. M. Ahmadiantehrani for obtaining TEM images, and W. Thompson for assistance on GPC data acquisition. Finally, we would like to thank Dr. Saw-Wai Hla and Dr. Li (Argonne National Laboratory) for insightful STM discussions.

## ■ REFERENCES


(1) Novoselov, K. S.; Geim, A. K.; Morozov, S. V.; Jiang, D.; Zhang, Y.; Dubonos, S. V.; Grigorieva, I. V.; Firsov, A. A. *Science* **2004**, *306*, 666.

(2) Blake, P.; Brimicombe, P. D.; Nair, R. R.; Booth, T. J.; Jiang, D.; Schedin, F.; Ponomarenko, L. A.; Morozov, S. V.; Gleeson, H. F.; Hill, E. W.; Geim, A. K.; Novoselov, K. S. *Nano Lett.* **2008**, *8*, 1704.

(3) Geim, A. K.; Novoselov, K. S. *Nat. Mater.* **2007**, *6*, 183.

(4) Chen, L.; Hernandez, Y.; Feng, X.; Müllen, K. *Angew. Chem., Int. Ed.* **2012**, *51*, 7640.

(5) Ma, L.; Wang, J.; Ding, F. *ChemPhysChem* **2013**, *14*, 47.

(6) Bai, J.; Huang, Y. *Mater. Sci. Eng., R* **2010**, *70*, 341.

(7) Terrones, M.; Botello-Méndez, A. R.; Campos-Delgado, J.; López-Urías, F.; Vega-Cantú, Y. I.; Rodríguez-Macías, F. J.; Elías, A. L.; Muñoz-Sandoval, E.; Cano-Márquez, A. G.; Charlier, J.-C.; Terrones, H. *Nano Today* **2010**, *5*, 351.

(8) Han, M. Y.; Özyilmaz, B.; Zhang, Y.; Kim, P. *Phys. Rev. Lett.* **2007**, *98*, 206805.

(9) Chen, Z.; Lin, Y.-M.; Rooks, M. J.; Avouris, P. *Phys. E* **2007**, *40*, 228.

(10) Tapasztó, L.; Dobrik, G.; Lambin, P.; Biró, L. P. *Nat. Nanotechnol.* **2008**, *3*, 397.

(11) Jiao, L.; Zhang, L.; Wang, X.; Diankov, G.; Dai, H. *Nature* **2009**, *458*, 877.

(12) Kosynkin, D. V.; Higginbotham, A. L.; Sinitskii, A.; Lomeda, J. R.; Dimiev, A.; Price, B. K.; Tour, J. M. *Nature* **2009**, *458*, 872.

(13) Cano-Márquez, A. G.; Rodríguez-Macías, F. J.; Campos-Delgado, J.; Espinosa-González, C. G.; Tristán-López, F.; Ramírez-González, D.; Cullen, D. A.; Smith, D. J.; Terrones, M.; Vega-Cantú, Y. I. *Nano Lett.* **2009**, *9*, 1527.

(14) Jiao, L.; Wang, X.; Diankov, G.; Wang, H.; Dai, H. *Nat. Nanotechnol.* **2010**, *5*, 321.

(15) Kosynkin, D. V.; Lu, W.; Sinitskii, A.; Pera, G.; Sun, Z.; Tour, J. M. *ACS Nano* **2011**, *5*, 968.

(16) Nakada, K.; Fujita, M.; Dresselhaus, G.; Dresselhaus, M. S. *Phys. Rev. B: Condens. Matter Mater. Phys.* **1996**, *54*, 17954.

(17) Bennett, P. B.; Pedramrazi, Z.; Madani, A.; Chen, Y.-C.; de Oteyza, D. G.; Chen, C.; Fischer, F. R.; Crommie, M. F.; Bokor, J. *Appl. Phys. Lett.* **2013**, *103*, 253114.

(18) Narita, A.; Feng, X.; Hernandez, Y.; Jensen, S. A.; Bonn, M.; Yang, H.; Verzhbitskiy, I. A.; Casiraghi, C.; Hansen, M. R.; Koch, A. H. R.; Fytas, G.; Ivasenko, O.; Li, B.; Mali, K. S.; Balandina, T.; Mahesh, S.; De Feyter, S.; Müllen, K. *Nat. Chem.* **2013**, *6*, 126.

(19) Vo, T. H.; Shekhirev, M.; Kunkel, D. A.; Morton, M. D.; Berglund, E.; Kong, L.; Wilson, P. M.; Dowben, P. A.; Enders, A.; Sinitskii, A. *Nat. Commun.* **2014**, *5*, 3189.

(20) Vo, T. H.; Shekhirev, M.; Lipatov, A.; Korlacki, R. A.; Sinitskii, A. *Faraday Discuss.* **2014**, *173*, 105.

(21) Vo, T. H.; Shekhirev, M.; Kunkel, D. A.; Orange, F.; Guinel, M. J. F.; Enders, A.; Sinitskii, A. *Chem. Commun.* **2014**, *50*, 4172.

(22) Yang, X.; Dou, X.; Rouhanipour, A.; Zhi, L.; Räder, H. J.; Müllen, K. *J. Am. Chem. Soc.* **2008**, *130*, 4216.

(23) Narita, A.; Feng, X.; Müllen, K. *Chem. Rec.* **2015**, *15*, 295.

(24) Narita, A.; Wang, X.-Y.; Feng, X.; Mullen, K. *Chem. Soc. Rev.* **2015**, *44*, 6616.

(25) Kim, K. T.; Jung, J. W.; Jo, W. H. *Carbon* **2013**, *63*, 202.

(26) Kim, K. T.; Lee, J. W.; Jo, W. H. *Macromol. Chem. Phys.* **2013**, *214*, 2768.

(27) Schwab, M. G.; Narita, A.; Osella, S.; Hu, Y.; Maghsoumi, A.; Mavrinsky, A.; Pisula, W.; Castiglioni, C.; Tommasini, M.; Beljonne, D.; Feng, X.; Müllen, K. *Chem. - Asian J.* **2015**, *10*, 2134.

(28) Schwab, M. G.; Narita, A.; Hernandez, Y.; Balandina, T.; Mali, K. S.; De Feyter, S.; Feng, X.; Müllen, K. *J. Am. Chem. Soc.* **2012**, *134*, 18169.

(29) Narita, A.; Verzhbitskiy, I. A.; Frederickx, W.; Mali, K. S.; Jensen, S. A.; Hansen, M. R.; Bonn, M.; De Feyter, S.; Casiraghi, C.; Feng, X.; Müllen, K. *ACS Nano* **2014**, *8*, 11622.

(30) Ormsby, J. L.; Black, T. D.; Hilton, C. L.; Bharat; King, B. T. *Tetrahedron* **2008**, *64*, 11370.

(31) Cai, J.; Ruffieux, P.; Jaafar, R.; Bieri, M.; Braun, T.; Blankenburg, S.; Muoth, M.; Seitsonen, A. P.; Saleh, M.; Feng, X.; Mullen, K.; Fasel, R. *Nature* **2010**, *466*, 470.

(32) Zhang, H.; Lin, H.; Sun, K.; Chen, L.; Zagranyarski, Y.; Aghdassi, N.; Duhm, S.; Li, Q.; Zhong, D.; Li, Y.; Müllen, K.; Fuchs, H.; Chi, L. *J. Am. Chem. Soc.* **2015**, *137*, 4022.

(33) Chen, Y.-C.; de Oteyza, D. G.; Pedramrazi, Z.; Chen, C.; Fischer, F. R.; Crommie, M. F. *ACS Nano* **2013**, *7*, 6123.

(34) Abdurakhmanova, N.; Amsharov, N.; Stepanow, S.; Jansen, M.; Kern, K.; Amsharov, K. *Carbon* **2014**, *77*, 1187.

(35) Liu, J.; Li, B.-W.; Tan, Y.-Z.; Giannakopoulos, A.; Sanchez-Sanchez, C.; Beljonne, D.; Ruffieux, P.; Fasel, R.; Feng, X.; Müllen, K. *J. Am. Chem. Soc.* **2015**, *137*, 6097.

(36) Han, P.; Akagi, K.; Federici Canova, F.; Mutoh, H.; Shiraki, S.; Iwaya, K.; Weiss, P. S.; Asao, N.; Hitosugi, T. *ACS Nano* **2014**, *8*, 9181.

(37) Talirz, L.; Ruffieux, P.; Fasel, R. *Adv. Mater.* **2016**, DOI: 10.1002/adma.201505738.

(38) Mamane, V.; Hannen, P.; Fürstner, A. *Chem. - Eur. J.* **2004**, *10*, 4556.

(39) Shaibu, B. S.; Lin, S.-H.; Lin, C.-Y.; Wong, K.-T.; Liu, R.-S. *J. Org. Chem.* **2011**, *76*, 1054.

(40) Matsuda, T.; Moriya, T.; Goya, T.; Murakami, M. *Chem. Lett.* **2011**, *40*, 40.

(41) Feng, X.; Pisula, W.; Müllen, K. *J. Am. Chem. Soc.* **2007**, *129*, 14116.

(42) Mukherjee, A.; Pati, K.; Liu, R.-S. *J. Org. Chem.* **2009**, *74*, 6311.

(43) Tovar, J. D.; Swager, T. M. *J. Organomet. Chem.* **2002**, *653*, 215.

(44) Goldfinger, M. B.; Swager, T. M. *J. Am. Chem. Soc.* **1994**, *116*, 7895.

(45) Yang, W.; Monteiro, J. H. S. K.; de Bettencourt-Dias, A.; Catalano, V. J.; Chalifoux, W. A. *Angew. Chem., Int. Ed.* **2016**, DOI: 10.1002/anie.201604741; *Angew. Chem.* **2016**, DOI: 10.1002/ange.201604741.

(46) Sproul, K. C.; Chalifoux, W. A. *Org. Lett.* **2015**, *17*, 3334.




DOI: 10.1021/jacs.6b03014
*J. Am. Chem. Soc.* 2016, 138, 9137−9144

(47) Moore, J. S.; Weinstein, E. J.; Wu, Z. *Tetrahedron Lett.* **1991**, *32*, 2465.
(48) Socrates, G. *Infrared and Raman characteristic group frequencies: Tables and charts*, 3 ed.; John Wiley & Sons, Ltd.: Chichester, 2004.
(49) Bloino, J. *J. Phys. Chem. A* **2015**, *119*, 5269.
(50) Verzhbitskiy, I.; De Corato, M.; Ruini, A.; Molinari, E.; Narita, A.; Hu, Y.; Schwab, M. G.; Bruna, M.; Yoon, D.; Milana, S.; Feng, X.; Müllen, K.; Ferrari, A. C.; Casiraghi, C.; Prezzi, D. *Nano Lett.* **2016**, *16*, 3442.
(51) Castiglioni, C.; Tommasini, M.; Zerbi, G. *Philos. Trans. R. Soc., A* **2004**, *362*, 2425.
(52) Lin, J.; Raji, A.-R. O.; Nan, K.; Peng, Z.; Yan, Z.; Samuel, E. L. G.; Natelson, D.; Tour, J. M. *Adv. Funct. Mater.* **2014**, *24*, 2044.
(53) Castillo-Martinez, E.; Carretero-Gonzalez, J.; Sovich, J.; Lima, M. D. *J. Mater. Chem. A* **2014**, *2*, 221.
(54) Kharissova, O. V.; Kharisov, B. I. *RSC Adv.* **2014**, *4*, 30807.
(55) Wen, Y.; He, K.; Zhu, Y.; Han, F.; Xu, Y.; Matsuda, I.; Ishii, Y.; Cumings, J.; Wang, C. *Nat. Commun.* **2014**, *5*, 4033.



DOI: 10.1021/jacs.6b03014
*J. Am. Chem. Soc.* 2016, 138, 9137−9144